



Identification of the trail-following pheromone receptor in termites

Reviewed Preprint

v1 • October 21, 2024

Not revised

Souleymane Diallo, Kateřina Kašparová, Josef Šulc, Jibin Johnny, Jan Křivánek, Jana Nebesářová, David Sillam-Dussès, Pavlína Kyjaková, Jiří Vondrášek, Aleš Machara, Ondřej Lukšan , Ewald Grosse-Wilde, Robert Hanus 

Institute of Organic Chemistry and Biochemistry of the Czech Academy of Sciences, Prague, Czech Republic • Czech University of Life Sciences, Prague, Czech Republic • Faculty of Science, Charles University, Prague, Czech Republic • Biology Centre of the Czech Academy of Sciences, Prague, České Budějovice, Czech Republic • University Sorbonne Paris Nord, 93430 Villetaneuse, France

 https://en.wikipedia.org/wiki/Open_access

 Copyright information

eLife Assessment

This **important** study presents the first identification of the odorant receptor for the trail pheromone in termites. The evidence supporting the conclusions is **compelling**, with state-of-the-art neurophysiological and genetic methods. The work will be of broad interest in multiple disciplines, such as entomology, chemical ecology, and sensory physiology.

<https://doi.org/10.7554/eLife.101814.1.sa3>

Abstract

Chemical communication is the cornerstone of eusocial insect societies since it mediates the social hierarchy, division of labor, and concerted activities of colony members. The chemistry of social insect pheromones received considerable attention in both major groups of social insects, the eusocial Hymenoptera and termites. By contrast, current knowledge on molecular mechanisms of social insect pheromone detection by odorant receptors (ORs) is limited to hymenopterian social insects and no OR was yet functionally characterized in termites, the oldest eusocial insect clade. Here, we present the first OR deorphanization in termites. Using the data from antennal transcriptome and genome of the termite *Prorhinotermes simplex* (Rhinotermitidae), we selected 4 candidate OR sequences, expressed them in Empty Neuron *Drosophila*, and functionally characterized using single sensillum recording (SSR) and a panel of termite semiochemicals. In one of the selected ORs, PsimOR14, we succeeded in obtaining strong and reliable responses to the main component of *P. simplex* trail-following pheromone, the monocyclic diterpene neocembrene. PsimOR14 showed a narrow tuning to neocembrene; only one additional compound out of 72 tested (geranylgeraniol) generated non-negligible responses. Subsequently, we used SSR and *P. simplex* workers to identify the olfactory sensillum specifically responding to neocembrene, thus likely expressing *PsimOR14*. We report on homology-based modelling of neocembrene binding by PsimOR14 and show how different ligands impact the receptor dynamicity using molecular dynamics simulations. Finally, we demonstrate that *PsimOR14* is significantly more expressed in workers than in soldiers, which correlates with higher sensitivity of workers to neocembrene.

Introduction

Chemical communication is the cornerstone of eusocial insect societies. It mediates the social hierarchy and division of labor, social cohesion and concerted activities of colony members. Major clades of eusocial insects have convergently evolved chemical signals acting in similar social contexts, as manifested by the presence of queen pheromones, trail-following pheromones, alarm pheromones, sex pheromones, food-marking pheromones, and colony and/or caste recognition cues in eusocial Hymenoptera and in termites, in spite of different glandular origins and diverse chemistries of these signals in the two evolutionarily distant insect clades (Leonhardt et al., 2016 [↗](#)).

Chemical diversity of pheromone communication in termites (Isoptera) has been extensively studied during the past decades. This applies in particular to trail-following pheromones (TFPs) and sex-pairing pheromones (SPPs), whose current knowledge covers all major termite lineages and allows for evolutionary reconstructions of pheromone chemistry. In contrast to the overall complexity of chemical communication in termite colonies, the chemical diversity of TFPs and SPPs is relatively modest, with only a handful of compounds acting as these pheromones or as components thereof across the phylogeny of Isoptera. Moreover, due to common evolutionary origin of trail-following behavior and sex-pairing behavior, the same compounds may be parts of both SPPs and TFPs in individual species and lineages, adding yet another level of pheromone parsimony (Bordereau & Pasteels, 2011 [↗](#)). In the basal lineages Mastotermitidae + Teletisoptera, linear and branched primary alcohols and aldehydes with 13 or 14 carbons play the role of TFPs and SPPs. Major evolutionary transition takes place in Kalotermitidae + Neoisoptera (Icoisoptera, over 98% of living species), in which unbranched C₁₂ fatty alcohols with one, two or three double bonds became almost universally present in both pheromone types as single components or in species-specific mixtures (Bagnères & Hanus, 2015 [↗](#); Bordereau & Pasteels, 2011 [↗](#); Mitaka & Akino, 2021 [↗](#); Sillam-Dussès, 2010 [↗](#)). Within Neoisoptera, the recently diversified group containing over 70% of modern termite species, this striking conservativeness of TFP and SPP components is in part enriched by occasional occurrence of terpenoids, such as the cyclic diterpene hydrocarbons neocembrene and trinervitatriene (Bordereau & Pasteels, 2011 [↗](#); Mitaka & Akino, 2021 [↗](#)).

Since the identification of the multigene family of insect odorant receptors (ORs) expressed in antennae and maxillary palps of *Drosophila melanogaster* (Clyne et al., 1999 [↗](#)), neurophysiology of insect olfaction underwent a great progress manifested by phylogenetic reconstructions of their evolution across insect taxa, functional characterizations (deorphanisations) of many ORs and ultimately by structural characterizations (Butterwick et al., 2018 [↗](#); del Mármol et al., 2021 [↗](#)). Even though the insect ORs have seven transmembrane domains (TMDs) like the ORs known from vertebrates, they do not share many tangible sequence similarities. Insect ORs have an inverted membrane topology in the dendrites of olfactory sensory neurons compared to vertebrate ORs (Benton et al., 2006 [↗](#); Clyne et al., 1999 [↗](#)) and unlike the vertebrate ORs known to act as GPCR receptors, insect ORs function as odorant-gated ion channels (Sato et al., 2008 [↗](#); Wicher et al., 2008 [↗](#)). While the ORs from the basal wingless insect lineage Archaeognatha are organized as homotetramers (del Mármol et al., 2021 [↗](#)) and lack a coreceptor protein (Brand et al., 2018 [↗](#)), ORs of all other Insecta including the apterygote clade of Zygentoma form heteromeric complexes with a highly conserved coreceptor protein (ORCo) (Brand et al., 2018 [↗](#); Butterwick et al., 2018 [↗](#); Larsson et al., 2004 [↗](#); Sato et al., 2008 [↗](#)).

The OR repertoire is greatly variable across Insecta and ranges from units in the wingless Archaeognatha and basal winged order Odonata to tens or hundreds ORs identified in most other flying insects, the record holders being Hymenoptera, especially ants with up to five hundred identified ORs (Engsontia et al., 2015 [↗](#); Robertson, 2019 [↗](#); Yan et al., 2020 [↗](#)). Insect ORs often

lack a clear orthology pattern across phylogeny and the OR family evolved via rapid birth-and-death process, accompanied by multiple gene duplications, pseudogenizations, and losses. Lineage-specific expansions, together with a considerable variability in OR ligand specificities (from broad to narrow tuning) allow for a rapid response of olfactory system to ecological and life history changes (Andersson et al., 2015 [↗](#); Benton, 2015 [↗](#); Nei & Rooney, 2005 [↗](#); Robertson, 2019 [↗](#)). Ecology-driven plasticity in OR evolution has been convincingly demonstrated by comparisons of specialist vs. generalist insects, the former often having much lower repertoires of ORs and other chemosensory proteins such as gustatory (GR) and ionotropic receptors (IR) (Robertson, 2019 [↗](#)). Another plausible example of OR evolution responding to life history traits is that of eusocial Hymenoptera; their complex chemical communication linked with eusociality is accompanied by striking OR family expansion (Engsontia et al., 2015 [↗](#); Legan et al., 2021 [↗](#); McKenzie et al., 2016 [↗](#); Pask et al., 2017 [↗](#); Zhou et al., 2015 [↗](#)).

The knowledge on OR structure and function, ligand specificities and tuning has historically been obtained mainly from studies on holometabolan insects using various heterologous deorphanisation systems, and eusocial Hymenoptera received considerable attention with multiple ORs being deorphanized in ants (Pask et al., 2017 [↗](#); Slone et al., 2017 [↗](#)) and the honey bee (e.g., Gomez Ramirez et al., 2023 [↗](#); Wanner et al., 2007 [↗](#)). Only recently this bias was in part compensated by successful OR deorphanisations in more basal taxa, e.g., the basal insect lineage Archaeognatha (del Marmol et al., 2021 [↗](#)) or the hemimetabolous aphids (Zhang et al., 2017 [↗](#), 2019 [↗](#)). Within Polyneoptera, OR detecting the aggregation pheromone was identified in the migratory locust (Guo et al., 2020 [↗](#)) and very recently a comprehensive deorphanization effort identified multiple narrowly tuned locust ORs responsible for environmental cues recognition (Chang et al., 2023 [↗](#)). No attempt was yet made to functionally characterize the ORs in termites, the oldest clade of social insects, which evolved roughly 140 my within Polyneoptera as an internal group of cockroaches (Blattodea) (Buček et al., 2019 [↗](#); Evangelista Dominic et al., 2019 [↗](#)). Diversity of termite ORs and other chemoreceptor proteins was previously inferred from genome assemblies (Harrison et al., 2018 [↗](#); Terrapon et al., 2014 [↗](#)) or whole-body transcriptomes (Mitaka et al., 2016 [↗](#)). Recently, we performed a comprehensive search for chemosensory protein repertoire in workers of three termite species belonging to different families using the antennal transcriptomes (Johnny et al., 2023 [↗](#)). At the first view, the correlation between the social evolution and OR diversity depicted for eusocial Hymenoptera does not hold in termites, because termite ORs are organized in relatively conserved, highly orthologous pattern and their total numbers, ranging from 28 to 69 (Johnny et al., 2023 [↗](#); Terrapon et al., 2014 [↗](#)), are quite low and even lower than OR repertoire of the solitary cockroach *Blattella germanica* (Harrison et al., 2018 [↗](#)).

Here, we report on the first deorphanisation of an OR from termites, more specifically on the OR for the major component of the TFP in *Proterhinotermes simplex* (Rhinotermitidae), the cyclic diterpene neocembrene. We take advantage of the good knowledge on the chemical ecology of this species, ranging from the chemistry of soldier-produced defensive compounds (Hanus et al., 2006 [↗](#); Jirošová et al., 2017 [↗](#); Piskorski et al., 2007 [↗](#)) to the chemical identity of TFPs and SPPs. The sex-pairing behavior is mediated by the C₁₂ alcohol (3Z,6Z,8E)-dodecatrien-1-ol (Hanus et al., 2009 [↗](#)). The same compound also serves as the minor component of TFP, the major component being neocembrene (Sillam-Dussès et al., 2009 [↗](#)). We build on the annotated repertoire of 50 ORs from *P. simplex* antennal transcriptome (Johnny et al., 2023 [↗](#)) and our additional *P. simplex* sequencing data, i.e., caste-specific head transcriptomes, draft genome assembly and long-term laboratory culture of the species in multiple colonies. We select four *P. simplex* candidate OR sequences from reconstructed termite OR phylogeny, study their function by means of the Empty Neuron *Drosophila in vivo* expression system and single-sensillum recording (SSR) using panels of potential ligands with biological relevance for termites. We report on strong and selective response of PsimOR14 to neocembrene. In addition, we identify the *P. simplex* olfactory sensillum specifically responding to neocembrene and document worker caste-biased expression of PsimOR14 accompanied by significantly higher sensitivity to neocembrene, compared to *P. simplex* soldiers.

Results

Phylogenetic reconstruction and candidate OR selection

In the first step, we reconstructed the phylogeny of termite ORs using previously published OR protein sequences from two species in combination with our antennal transcriptome data on workers from three species (Johnny et al., 2023 [DOI](#)), including *P. simplex*. The resulting phylogenetic tree, shown in **Fig. 1** [DOI](#) and Supplementary Fig. S1, revealed an expected highly orthologous pattern, with OR sequences from all five termite species being represented in most sub-branches and with relatively few species-specific expansions. Beside two basally situated monophyletic lineages consisting of only a few OR sequences, the remainder of the tree was organized into two large sister clusters rich in ORs from all studied species. From the 50 *P. simplex* ORs mapped on the tree, we selected for the first deorphanization attempts 4 ORs (PsimOR9, 14, 30 and 31) distributed at different branches across the phylogenetic diversity of termite ORs (**Fig. 1A** [DOI](#)). Their sequences were used for transgenic *D. melanogaster* generation and SSR screening.

Functional characterization of *P. simplex*

ORs in *D. melanogaster* ab3 sensillum

We expressed the four selected *P. simplex* ORs in the recently improved version of the *Drosophila melanogaster* Empty Neuron system (Chahda et al., 2019 [DOI](#)); the crossing scheme for fly generation adapted from Gonzales et al. (Gonzalez et al., 2016 [DOI](#)) is shown in Supplementary Fig. S2. Spontaneous SSR firing rates of the four transgenic lines showed an expected pattern with no abnormal bursts, indicating that the ORs were functional. The flies were first subjected to SSR screening with Panel 1, consisting of 17 semiochemicals relevant to termite chemical communication and structurally related compounds. As shown in **Fig. 2A** [DOI](#), PsimOR9 and PsimOR30 did not provide any strong response to any of the tested compounds, while PsimOR31 broadly and weakly responded to several compounds. By contrast, PsimOR14 systematically and strongly responded to stimulations by the monocyclic diterpene hydrocarbon neocembrene. Additionally, a moderate PsimOR14 response was also recorded for the linear diterpene alcohol geranylgeraniol, while all other compounds in the panel, including three other terpenoids, only elicited weak or no responses (**Fig. 2A** [DOI](#), Supplementary Tables S1–S4).

We then compared the responses of *Drosophila* ab3 sensillum in PsimOR14 expressing flies with those of *W*¹¹¹⁸ flies. As evidenced in **Fig. 2B** [DOI](#), *W*¹¹¹⁸ ab3 sensillum did not show any significant neuronal response to Panel 1 compounds, while the transgenic PsimOR14 line generated an average Δ spike number of >50 spikes/s for neocembrene and a minor secondary response of ~25 Δ spikes/s for geranylgeraniol. Characteristic responses for both lines to the two compounds are depicted in **Fig. 2C** [DOI](#). In the next step, we tested the dose-response behavior of PsimOR14 flies to neocembrene, which showed an exponentially increasing neuronal response over the range of 0.01–10 ng to ED50 = ~24 ng and a lack of saturation at the dose of 500 ng (**Fig. 2D** [DOI](#), Supplementary Tables S5, S6).

PsimOR14 is narrowly tuned to neocembrene, the main trail-following pheromone component

To further address the specificity of PsimOR14 tuning, we tested three additional panels containing 56 frequently occurring insect semiochemicals from various chemical classes. As shown in **Fig. 3A** [DOI](#), none of these compounds, including multiple terpenoids (mono-, sesqui-, di-), generated a strong response, suggesting a narrow tuning of PsimOR14 to neocembrene. The narrow tuning of PsimOR14 is evident also from the tuning curve depicted in **Fig. 3B** [DOI](#), with the

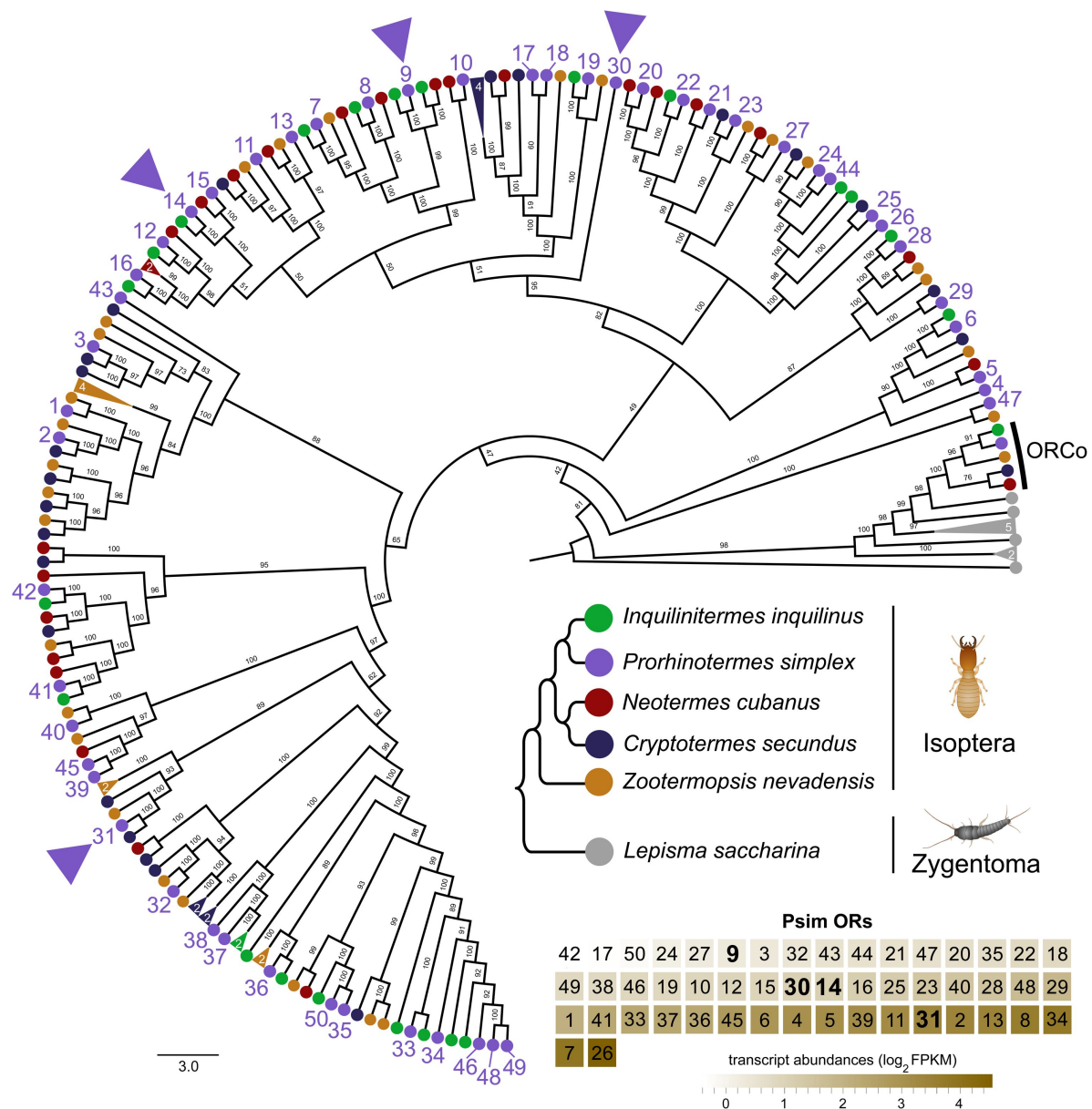


Fig. 1.

Phylogenetic reconstruction of termite ORs

The tree is based on 182 protein sequences from five species of termites and the bristletail *Lepisma saccharina* as a basal insect outgroup, and also includes the sequences of OR co-receptor (OrCo). The topology and branching supports were inferred using the IQ-TREE maximum likelihood algorithm with the JTT+F+R8 model and supported by 10,000 iterations of ultrafast bootstrap approximation. Protein sequences of termite ORs can be found under the same labeling in [Johnny et al. \(2023\)](#). *Lepisma saccharina* sequences are listed in [Thoma et al. \(2019\)](#). Arrowheads highlight the four ORs from *Prorhinotermes simplex* selected for functional characterization. Fully annotated version of the tree is provided as Supplementary Fig. S1. Heatmap shows the abundances of 50 OR transcripts identified in the RNAseq data from *P. simplex* antennae available in NCBI SRA archive under accession SRX17749141.

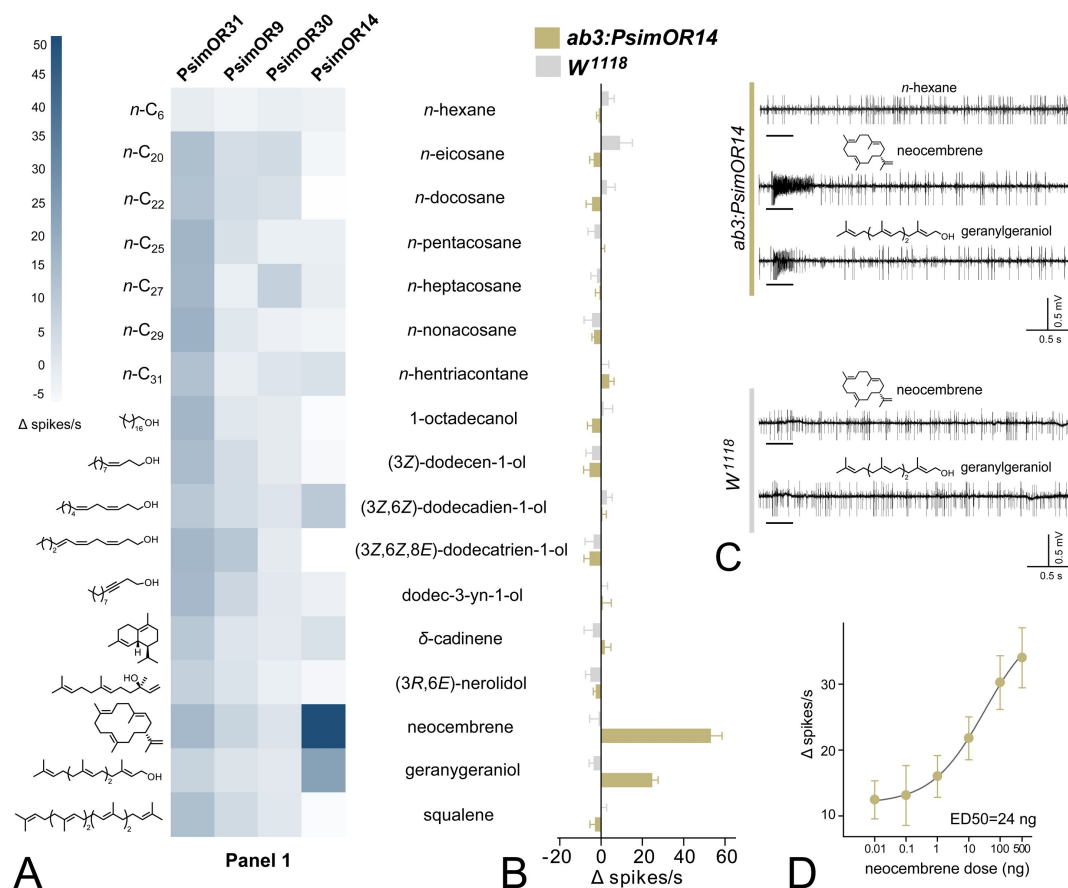


Fig. 2.

SSR responses of transgenic *D. melanogaster* ab3 sensillum expressing PsimOR9, 14, 30 and 31 to the panel of 17 volatiles with biological relevance for termites

A Heatmap showing the average responses of the four ORs as Δ spikes/s from 3–6 independent replicates. **B.** Comparison of SSR responses of transgenic *Drosophila melanogaster* ab3A neurons expressing PsimOR14 (*ab3A:PsimOR14*) and *W*¹¹¹⁸ *D. melanogaster*. The bars show the average Δ spikes/s values from five independent replicates \pm SEM. **C.** Characteristic SSR traces of *ab3A:PsimOR14* and *W*¹¹¹⁸ flies for 1 μ g dose of neocembrene and geranylgeraniol. **D.** Dose response curve of *ab3A:PsimOR14* SSR responses to neocembrene. The graph shows average Δ spikes/s values \pm SEM based on nine replicates (8 in case of 100 ng and 4 in case of 500 ng stimulations). The curve fit and ED50 value were calculated using log(agonist) vs. response non-linear algorithm with least square fit method and the constraint of minimal response > 0. The raw data for all graphs is provided in Supplementary Tables S1–S6.

receptor lifetime sparseness value 0.89 (Supplementary Tables S7–S9). These results suggest that PsimOR14 is a pheromone receptor adaptively tuned to neocembrene, which is the main component of the trail-following pheromone in the genus *Prorethina*.

Identification of *P. simplex* olfactory sensillum involved in neocembrene detection

Our next goal was to identify the antennal olfactory sensillum responsible for neocembrene detection by *P. simplex* workers by combination of SSR measurements with SEM and HR-SEM imaging. Since no previous study reported SSR responses of termite olfactory sensilla to pheromones and environmental cues, we decided to search for the neocembrene-detecting sensillum on the last flagellomere, known to harbor by far the most sensilla in termite workers (Castillo et al., 2021 [DOI](#)).

SEM mapping of the distal antennal segment revealed multiple types of multiporous trichoid and basiconic sensilla with potential olfactory function (Fig. 4A [DOI](#)). In SSR experiments using the termite-relevant compounds from Panel 1, we obtained strong response to both neocembrene and geranylgeraniol from a short multiporous grooved sensillum situated in the apical part of the last segment. Detailed retrieval using HR-SEM allowed us to distinguish five types of multiporous grooved sensilla according to their wall structure, overall shape, length, and shape of the sensillar tip. The neocembrene-detecting sensillum belongs to S I type according to this classification (Fig. 4A, B [DOI](#)). Detailed view on spontaneous firing pattern of the neocembrene-detecting sensillum revealed three different spike amplitudes (Fig. 4C [DOI](#)), suggesting the potential presence of as many as three olfactory sensory neurons (a–c). Comparison with spike amplitudes upon neocembrene and geranylgeraniol stimulation then indicated that the responses correspond to the neuron labeled as b.

The response spectrum of neocembrene sensillum to Panel 1 was markedly similar to that of ab3A neuron of PsimOR14-expressing *Drosophila* (Fig. 5A [DOI](#)). None of the compounds elicited higher average responses than 10 Δ spikes/s, except for neocembrene and geranylgeraniol; their average Δ spikes/s were even slightly higher than those of heterologously expressed PsimOR14, reaching ~65 and ~29, respectively (Fig. 5A, B [DOI](#)). Likewise, the dose-response experiment with neocembrene indicated a higher sensitivity threshold and lower ED50 = 0.016 ng (Fig. 5C [DOI](#), Supplementary Tables S10, S11).

PsimOR14 gene and protein structure, protein modeling, ligand docking, and MM-PBSA molecular dynamics (MD) simulations

Mapping the *PsimOR14* transcript sequence on *P. simplex* draft genome revealed that the gene consists of six exons and is situated on the same locus and in close vicinity of *PsimOR15*, with which it shares the exon-intron boundaries, suggesting a recent diversification of the two genes via duplication, as also supported by their high sequence similarity (Fig. 6A [DOI](#), Fig. 1 [DOI](#)). Transcript (Fig. 6B [DOI](#)) and protein (Fig. 6C [DOI](#)) structures of PsimOR14 showed the presence of seven TMDs with the largest extracellular loop connecting TMD3 and TMD4 and the longest intracellular loop between TMD4 and TMD5.

The initial PsimOR14 model was obtained using AlphaFold 2. After minimization and annealing of six molecular dynamics replicas, the structure with the lowest potential energy was selected for docking while assuming a homologous binding region to that reported in the structural characterization of MhOR5 from *Machilis hrabei* (7LIG) (del Mármol et al., 2021 [DOI](#)). The identified binding site, based on the superposition of 7LIG and our PsimOR14 model, is shown in Fig. 6D [DOI](#). For docking and MD simulations, three terpenoid ligands were selected from Panel 1, i.e., the best PsimOR14 agonists neocembrene and geranylgeraniol, and a weak agonist squalene (see Fig. 2 [DOI](#)).

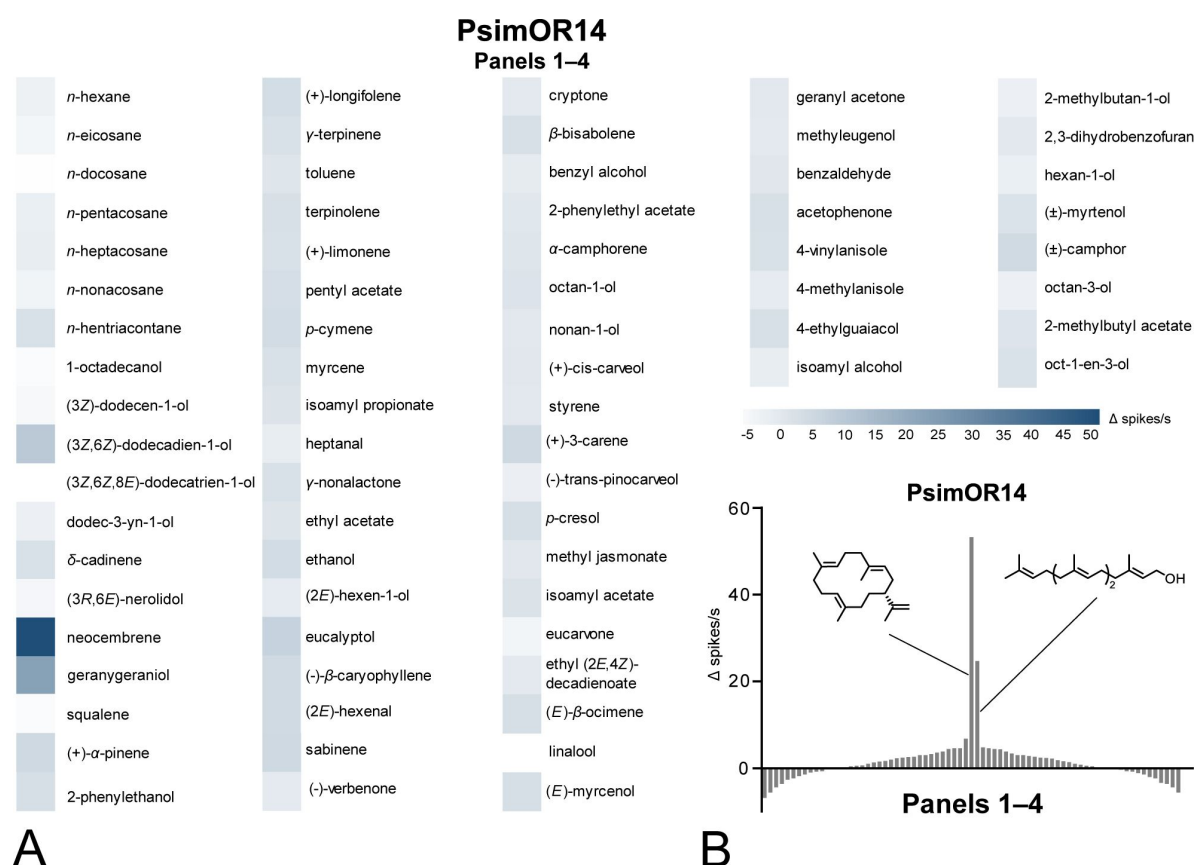


Fig. 3.

SSR responses of transgenic *D. melanogaster* ab3 sensillum expressing PsimOR14 to the complete set of 73 compounds (Panels 1–4)

A. Heatmap showing the average responses as Δ spikes/s from 3–6 independent replicates. **C.** Tuning curve of PsimOR14 for the 73 compounds contained in panels 1–4. The raw data is provided in Supplementary Tables S7–S9.

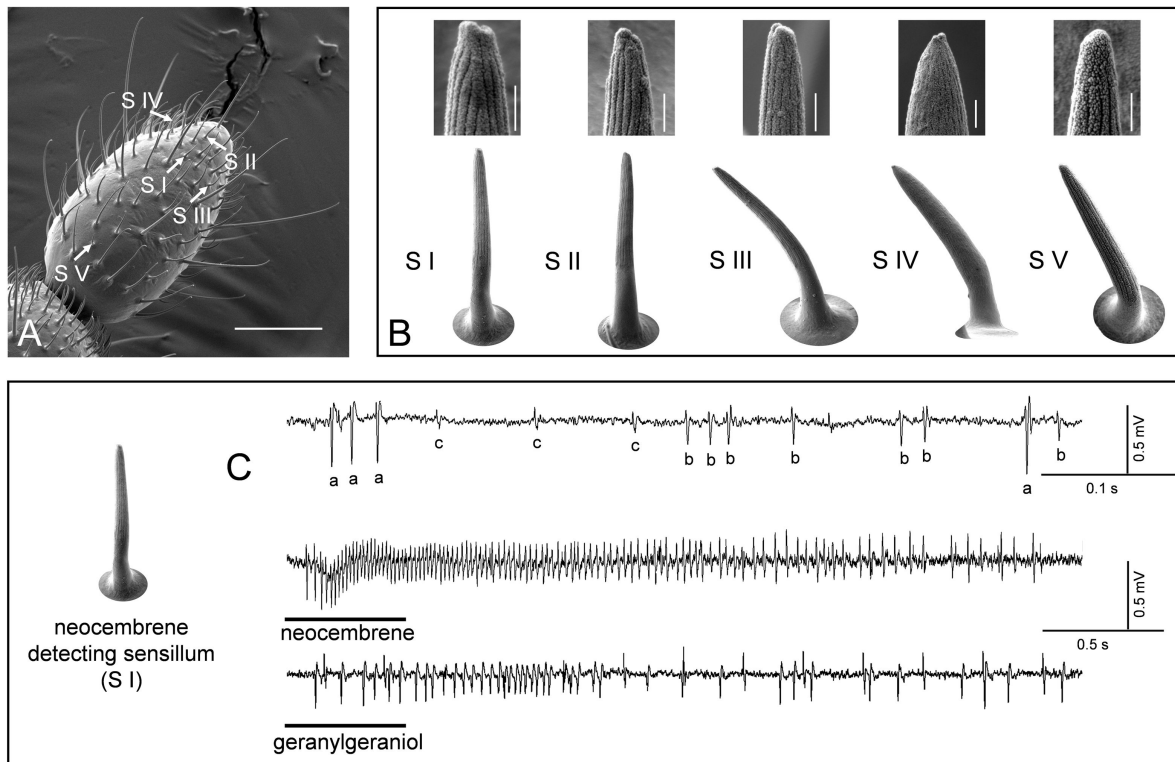


Fig. 4.

Distribution of olfactory sensilla on the last antennal segment of *P. simplex* workers

A. Arrows show the localization of selected representatives of the five distinguished multiporous grooved sensilla types (S I–V) on a SEM photograph of the last flagellomere. Scale bar represents 50 μm . **B.** Detailed view on the five identified types of multiporous grooved sensilla using HR-SEM. Scale bar represents 500 nm. **C.** Detailed view on SSR traces of spontaneous spikes from the neocembrene-detecting sensillum of S I type, showing spikes of three different amplitudes. **D.** SSR traces recorded on neocembrene-detecting sensillum for neocembrene and geranylgeraniol.

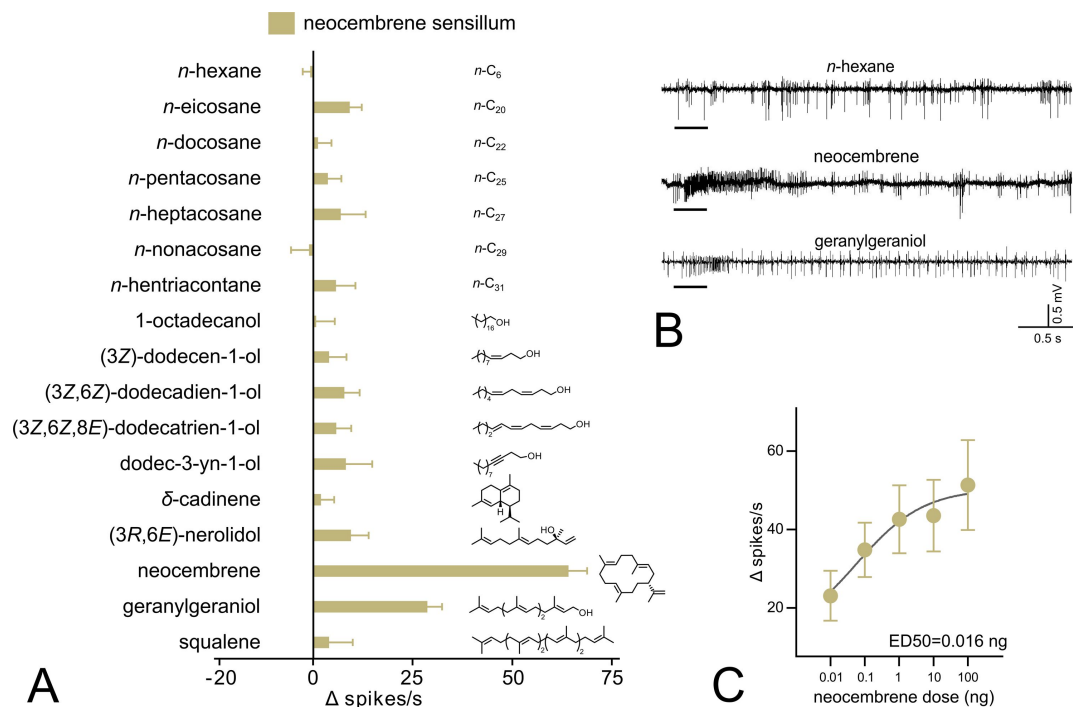


Fig. 5.

SSR responses of the neocembrene-detecting SB I sensillum on the last flagellomere of *P. simplex* worker

A SSR responses to the main panel of volatiles with biological relevance for termites. The bars show the average Δ spikes/s values from 8–12 replicates \pm SEM. The raw data is provided in Supplementary Tables S10. **B.** Characteristic SSR traces of the neocembrene-detecting SB I sensillum for neocembrene and geranylgeraniol. **C.** Dose response curve of the SSR responses to neocembrene by the SB I sensillum. The graph shows average Δ spikes/s values \pm SEM based on 9–11 replicates. The curve fit and ED50 value were calculated using log(agonist) vs. response non-linear algorithm with least square fit method and the constraint of minimal response > 0. The raw data is provided in Supplementary Table S11.

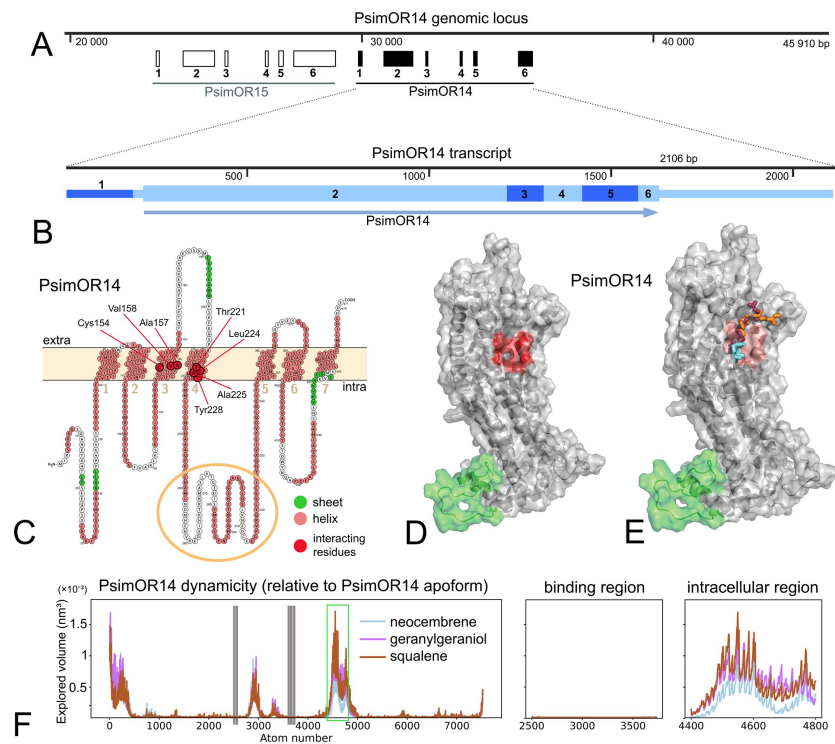


Fig. 6.

PsimOR14 gene, transcript and protein structures, docking and MD simulations

A Genomic locus containing *PsimOR14* and *PsimOR15*. *PsimOR14* gene consists of 1 non-coding and 5 protein coding exons. **B**. *PsimOR14* transcript with 6 exons represented as blue boxes with variable height according to protein-coding (higher) or untranslated (smaller) regions. ORF is marked by blue arrow. **C**. Transmembrane architecture of *PsimOR14*. In red are shown seven residues interacting with each of the three studied ligands, the green ellipse shows the intracellular flap the most impacted by ligand binding. **D**. Modelled apoform of *PsimOR14*. Red region denotes the binding site identified via docking, green region represents the intracellular flap region. **E**. Holoforms of *PsimOR14* with sticks representing ligands without hydrogens (cyan = neocembrene, red = geranylgeraniol, orange = squalene). **F**. Relative mean volumes explored by atoms of *PsimOR14* per simulation step when liganded with neocembrene, geranylgeraniol and squalene. *PsimOR14* apoform represents the baseline zero. Gray lines show the binding site region, the green line delimits the intracellular flap the most affected by ligation. The whole *PsimOR14* protein shown on the left, detail on the binding region in the middle and the intracellular flap on the right. Nucleotide and protein sequences of *PsimOR14* are provided in Supplementary Table S12 and as NCBI entry under accession OR921181.

Their structures were parametrized using the CgenFF 4.6 forcefield via CHARMM-GUI and docked into the binding region of PsimOR14 using a flexible ligand docking algorithm. All the final binding poses occupy the same ligand binding site, and only the best-ranked pose for each ligand was selected for further analysis. Dockings are visualized in [Fig. 6E](#), the final scores of the best-ranked poses are shown in [Table 1](#). Based on the composition of the scores, we hypothesized that primarily Van der Waals interactions facilitate the binding, providing more possibilities to adapt a similar energy profile for the bound ligand.

Surprisingly, the ranking of the predicted binding strength squalene > geranylgeraniol > neocembrene did not correspond to the biological effect of the agonists observed in SSR assays (neocembrene > geranylgeranyl > squalene) ([Table 1](#)). Per-residue decomposition results (Supplementary Tables S13, S14) showed that all three ligands bind two hydrophobic patches made out of residues from TMD3 and TMD4 (Cys154, Ala157, Val158; Thr221, Leu224, Ala225, Tyr228). Neocembrene binds only these patches, while geranylgeraniol also interacts with Gly161, Phe162, Ile165, Ile217, and Val220. Squalene, being the largest ligand, additionally contacts Met37, Val166, and Phe169. Thus, the predicted binding strength order may be due to the increasing number of stabilizing contacts between the hydrophobic binding region and hydrophobic ligands, without being necessarily translated onto the biological effect on the receptor function based on the receptor selectivity.

By contrast, our subsequent analysis of PsimOR14 dynamic behaviour revealed an interesting impact of ligand binding on the dynamicity of the protein, especially in its intracellular region. Using a proprietary protocol and the convex hull algorithm, we analysed changes in per-atom dynamic behaviour across different forms. By tracing three-dimensional polytopes of atomic positions over time, we approximated the volume per step and arrived at a scalar V_{ex} describing the total dynamicity of a region or the whole protein. As shown in [Table 1](#) and [Fig. 6F](#), the binding of the ligands has a strong effect on the dynamicity especially in the intracellular protein region manifested by relative dynamicity ordered as squalene > geranylgeranyl > neocembrene. Thus, the strength of the effect of different ligands on the intracellular region matches the functional SSR experiments and demonstrates the allosteric effect transferring the distribution of the binding to the protein periphery.

Caste-biased PsimOR14 expression and antennal sensitivity to neocembrene

We next decided to compare the expression pattern of PsimOR14 between *P. simplex* workers and soldiers, along with the sensitivity of the two castes to its preferred ligand, neocembrene. Differential expression analyses of the head RNAseq data from workers and soldiers revealed that PsimOR14 is significantly more expressed in workers, being among 10 of the most differentially expressed ORs ([Fig. 7A](#), Supplementary Table S15). Subsequent EAG measurements were in line with this observation and indicated significantly stronger responses to neocembrene in workers ($p=0.012$) ([Fig. 7B](#), Supplementary Table S16).

Discussion

Identification of PsimOR14 as a pheromone receptor narrowly tuned to neocembrene, the main component of the TFP in *P. simplex*, represents the first deorphanisation of an odorant receptor in termites. In contrast to eusocial Hymenoptera, the molecular aspects of termite chemical communication and orientation remain largely understudied despite the systematic effort previously dedicated to unveil the chemical identity, glandular origin and biological functions of termite pheromones (Bagnères & Hanus, 2015; Bordereau & Pasteels, 2011; Mitaka & Akino, 2021; Sillam-Dussès, 2010). Current knowledge is limited to a few studies listing the termite

Table 1.

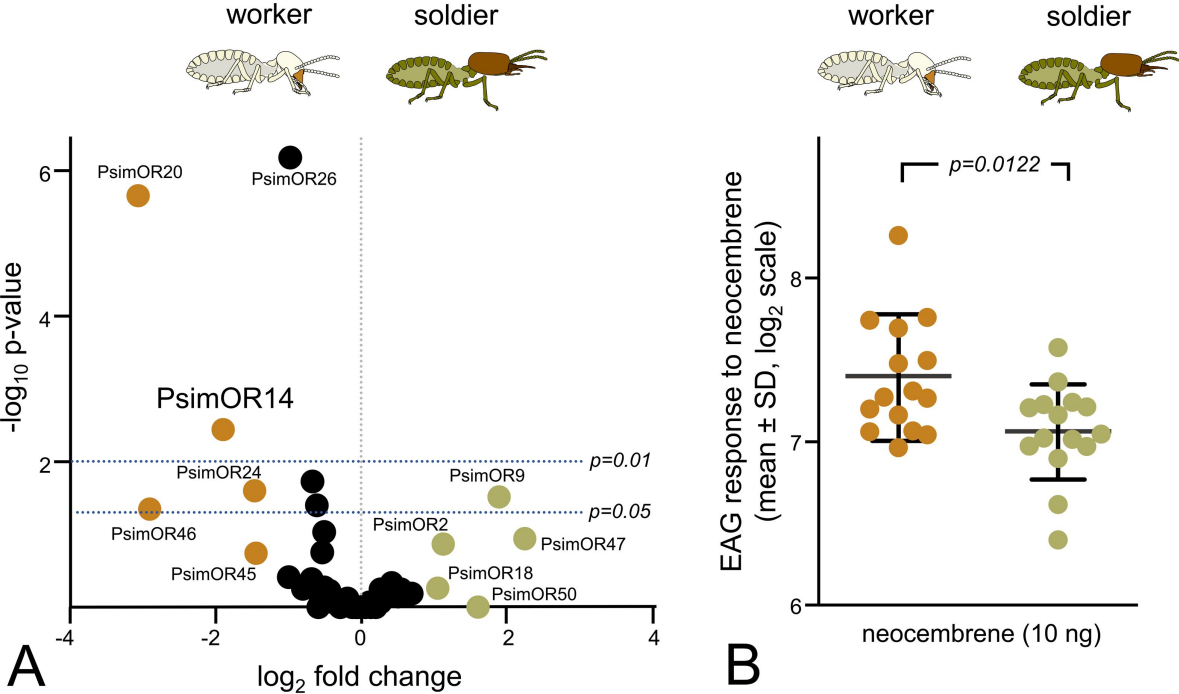
Docking scores, contributions of van der Waals and electrostatic forces and relative dynamicity values of PsimOR14 upon binding of neocembrene, geranylgeraniol and squalene

ligand	docking score	van der Waals interactions	electrostatic interactions	V_{protein} (nm ³)	$V_{\text{binding region}}$ (nm ³)	$V_{\text{intracellular region}}$ (nm ³)
apoform				4.47 ± 0.522	$2.88 \times 10^{-3} \pm 4.19 \times 10^{-4}$	0.185 ± 0.0862
neocembrene	-8.658	-19.777	-0.223	2.09 ± 0.603	$1.30 \times 10^{-3} \pm 2.92 \times 10^{-4}$	0.0527 ± 0.0394
geranylgeraniol	-8.331	-18.786	-11.137	1.98 ± 0.428	$1.08 \times 10^{-3} \pm 1.03 \times 10^{-4}$	0.0700 ± 0.0314
squalene	-10.09	-33.58	-0.589	1.9 ± 0.535	$1.02 \times 10^{-3} \pm 1.55 \times 10^{-4}$	0.0744 ± 0.0725

Fig. 7.

Caste comparison of *PsimOR14* expression and EAG responses between *P. simplex* workers and soldiers

A Volcano plot representing edgeR differential gene expression analysis of all 50 *P. simplex* ORs in RNAseq data from soldier and workers heads. Colored dots mark ORs reaching absolute value of log₂ fold change ≥ 1, horizontal lines represent p-value thresholds of 0.05 and 0.01. Numeric values of the edgeR and DESeq2 differential expression analysis are provided in Supplementary Table S15. **B**. EAG responses of whole antenna preparations of workers and soldiers to neocembrene at a dose of 10 ng (mean ± SD shown on log₂ scale). Inter-caste differences were compared using t-test on log₂-transformed data. Raw data is shown in Supplementary Table S16.



OR repertoire (Harrison et al., 2018 [↗](#); Johnny et al., 2023 [↗](#); Terrapon et al., 2014 [↗](#)), caste-specific OR expression (Mitaka et al., 2016 [↗](#)), or addressing the significance of ORCo for olfactory function (Castillo et al., 2022 [↗](#); Gao et al., 2020 [↗](#)).

Multiple evidence suggests that the complex communication and orientation demands in the colonies of eusocial Hymenoptera are facilitated by the greatly expanded repertoire of ORs, especially that of the 9-exon subfamily in ants and paper wasps participating in the detection of cuticular hydrocarbons (CHCs) as important cues in contact chemoreception of colony and caste identity and fertility status in eusocial insects (Engsontia et al., 2015 [↗](#); Legan et al., 2021 [↗](#); McKenzie et al., 2016 [↗](#); Pask et al., 2017 [↗](#); Zhou et al., 2015 [↗](#)). The 9-exon subfamily and the overall OR richness has been inherited by the extant eusocial Hymenoptera from the ancestor of Aculeata (McKenzie et al., 2016 [↗](#)), and also solitary aculeate taxa display large OR repertoires (Obiero et al., 2021 [↗](#)); this preadaptation might had been important for the repeated emergence of eusociality and the related complex communication. This is supported by the convergent simplification of OR array (including 9-exon genes) in parasitic ant taxa, along with the simplification of their behavioral repertoire (Jongepier et al., 2022 [↗](#)).

With their small numbers of ORs, termites clearly contradict the paradigm on eusociality as a driver of OR richness. In spite of the parsimony of their pheromone diversity, their chemical communication remains by far more complex than in solitary insects and includes pheromone components from a variety of chemical classes, including fatty-acyl derived alcohols and aldehydes, terpenoids, and, last, but not least, the CHCs. Independently of eusocial Hymenoptera, termites evolved an intricate communication system using CHCs as kin- and nestmate discrimination cues and as indicators of caste identity and fertility status (reviewed in Bagnères & Hanus, 2015 [↗](#); Mitaka & Akino, 2021 [↗](#)). Therefore, the termite social evolution apparently adopted a different trajectory to accommodate the needs of chemical communication, including the detection of CHCs. One of alternative scenarios springs from observations that termites possess an extraordinarily rich set of ionotropic receptors (IRs), reaching up to more than one hundred IRs in some species (Harrison et al., 2018 [↗](#); Johnny et al., 2023 [↗](#); Terrapon et al., 2014 [↗](#)), and 95 IRs identified in *P. simplex* (Johnny et al., 2023 [↗](#)). Even though the richness of IRs is shared by termites and their cockroach relatives, with *B. germanica* having the largest IR repertoire ever identified in insects (Robertson et al., 2018 [↗](#)), IRs underwent termite-specific expansions (Harrison et al., 2018 [↗](#); Johnny et al., 2023 [↗](#)). Since IRs have been shown to detect olfactory information (Benton et al., 2009 [↗](#)), it has been speculated that the diversification of IRs may account for the complexity of termite chemical communication, as indirectly supported by caste and sex-specific pattern of their expression in termites (Harrison et al., 2018 [↗](#)). This hypothesis remains to be experimentally verified.

Nevertheless, as we show here, the trail-following communication by means of TFP, having shared evolutionary origins with termite courtship communication (Bagnères & Hanus, 2015 [↗](#); Bordereau & Pasteels, 2011 [↗](#); Sillam-Dussès, 2010 [↗](#)), is mediated by an odorant receptor. This is in line with the previous observations in two termite species showing that ORCo silencing impairs their ability to follow the foraging trail (Gao et al., 2020 [↗](#)).

Neurophysiological characteristics of *D. melanogaster* ab3 neuron expressing *PsimOR14* showed expected patterns of spontaneous firing rates of units of Hz (6.87 ± 4.73 , mean \pm SD) and maximum firing rates of 90 spikes/s at the highest used neocembrene doses (1 μ g), though not reaching the reported maxima for ab3 responses with genuine and exogenous receptors, which may be well over 100 spikes/s (e.g., Chahda et al., 2019 [↗](#)). This suggests that *Drosophila* Empty Neuron system co-expressing with the exogenous OR the *Drosophila* ORCo is a suitable technique for termite OR characterizations. The apparently narrow tuning of *PsimOR14* to the cyclic diterpene hydrocarbon neocembrene, with receptor lifetime sparseness equal to 0.89, is typical for insect ORs adaptively shaped to detect pheromone components (pheromone receptors) or other volatiles with high biological importance, such as key food or host attractants (e.g., Carey et al., 2010 [↗](#); Fleischer &

Krieger, 2018 [\[4\]](#)). With average Δ spike/s over 20, the linear diterpene alcohol geranylgeraniol was the only other agonist with non-negligible response; none of the remaining compounds elicited a Δ spike of more than 7. This ranking is interesting because the set of tested panels contained multiple other compounds derived from terpenoid scaffold, and invited to speculate about conformational similarities between neocembrene and geranylgeraniol. Even more interestingly, another related terpene alcohol, the monoterpene linalool, had the biggest negative Δ spike score (-6.8) and the absolute spikes/s ranged from 0 to 5 (1.5 ± 1.9 , mean \pm SD), suggesting a possible inverse agonist function of linalool.

The SSR-based identification of neocembrene-sensing sensillum in *P. simplex* workers provided a response pattern to Panel 1 very similar to that of *PsimOR14*-expressing ab3 *Drosophila* sensillum, e.g., strong response to neocembrene, followed by geranylgeraniol, supporting independently the results obtained from transgenic *Drosophila*. No other important responses to termite pheromone components from the Panel 1, which also includes the minor *P. simplex* TFP component (3Z,6Z,8E)-dodecatrien-1-ol, were recorded, in spite of the likely presence of two additional olfactory neurons harbored in the neocembrene-detecting sensillum.

The basic *PsimOR14* protein architecture showed a pattern typical for insect ORs, having seven TMDs. Likewise, the docking experiments with three selected ligands (neocembrene, geranylgeraniol and squalene) identified a binding site defined by a binding pocket deep in the transmembrane region, homologous to that in previously studied insect ORs, and confirmed the nature of the ligand binding to mainly rely on hydrophobic interactions (e.g., del Mármol et al., 2021 [\[4\]](#); Pettersson & Cattaneo, 2023 [\[4\]](#); Yuvaraj et al., 2021 [\[4\]](#)). In case of *PsimOR14*, mainly the hydrophobic and aromatic residues from TMD3 and TMD4 interacted with the studied ligands, as also suggested for some previously studied insect ORs (e.g., del Mármol et al., 2021 [\[4\]](#); Yuvaraj et al., 2021 [\[4\]](#)).

Our computational analysis of *PsimOR14* ligand binding did not provide a straightforward image of the binding affinity score as the best proxy of the biological effect size. The binding affinity, typically quantified through scoring functions that estimate the binding Gibbs free energy, often correlates well with experimental data, and may be useful for understanding how inhibitors might block native ligand binding. Yet, in systems where ligand binding induces allosteric effects, as is the case of insect ORs (del Mármol et al., 2021 [\[4\]](#)), the simple binding affinity does not provide a complete picture on receptor signal transduction function.

Our MM/PBSA analysis confirmed that the weakest agonist squalene exhibits the highest binding affinity, followed by geranylgeranyl and the strongest agonist neocembrene. This at the first view contradictory observation is in fact consistent with the number of stabilizing contacts identified for each ligand, which correlates with the space occupied by the ligands and increases from neocembrene through geranylgeraniol to squalene. By contrast, molecular dynamics analysis revealed that the binding of ligands reduces the dynamicity of *PsimOR14*'s intracellular region in the order neocembrene > geranylgeraniol > squalene. This dynamic effect aligns with the experimental data showing that neocembrene has the most significant biological impact. These results underscore the importance of considering both binding affinity and allosteric effects when analyzing ligand-receptor interactions.

PsimOR14 does not belong to the most expressed *P. simplex* ORs (Fig. 1 [\[4\]](#)). However, interestingly, it is among those having the most caste-biased expression with significantly higher transcript abundance in antennae of workers compared to soldiers. Accordingly, also the electrophysiological responses of workers to neocembrene were significantly larger in workers. Termite soldiers are known to lay pheromone trails, to detect TFPs and to participate in foraging and field exploration in a number of termite species, though the behavioral patterns of soldiers and workers during these activities differ (Kaib, 1990 [\[4\]](#); Traniello, 1981 [\[4\]](#); Traniello & Busher, 1985 [\[4\]](#)). This has also been demonstrated in a close relative to our model, the congeneric species *Prorhinotermes*

inopinatus (Rupf & Roisin, 2008 [↗](#)). Yet, differences in sensitivity of termite workers and soldiers have not previously been addressed at the electrophysiological level. Caste-biased *PsimOR14* expression and neocembrene sensitivity may represent olfactory information filtering adaptive to the different tasks of the two castes, as documented, e.g., in ants (Caminer et al., 2023 [↗](#)).

Genus *Prorhinotermes* is the most basally situated termite taxon having a terpenoid component as a part of its TFP (or SPP) (Sillam-Dussès et al., 2009 [↗](#)). The acquisition of terpenoid pheromone components is undoubtedly due to the evolution of terpene biosynthesis in basal Neoisoptera or their ancestors, which is manifested by fascinating diversity of terpenoids produced by soldiers of Neoisoptera as defensive compounds (Gössinger, 2019 [↗](#)). In line with general observations on pheromone evolution (Steiger et al., 2010 [↗](#)), some of these terpenoid products of the soldier defensive frontal gland gained via exaptation a novel function of alarm pheromones (Dolejšová et al., 2014 [↗](#); Roisin et al., 1990 [↗](#); Šobotník et al., 2008 [↗](#), 2010 [↗](#)), and the cyclic diterpenes became part of SPPs and TFPs in some species by co-opting the terpenoid biosynthesis in exocrine glands dedicated to SPP and TFP production. Beside the occurrence of neocembrene in the sub-basal *Prorhinotermes*, it only occurs as TFP and SPP component in much later diverging representatives of the modern family Termitidae (formerly also higher termites). It is particularly frequent as trail-following pheromone and sex-pairing pheromone in the diversified subfamily Nasutitermitinae (Bordereau & Pasteels, 2011 [↗](#)). Because neocembrene is deemed to be the monocyclic precursor of the defensive polycyclic diterpenes produced by Nasutitermitinae soldiers, it is plausible that it gained the secondary pheromone role by expressing the responsible (unknown) terpene synthase in the pheromone glands (sternal gland of workers and soldiers for TFP, tergal and/or sternal glands of female imagoes for SPP). Once reliable genome or antennal transcriptome of Nasutitermitinae sequences become available, it would be of interest to search in these species for OR orthologs of *PsimOR14* and test whether they have retained the function of neocembrene detection.

Within the available *P. simplex* OR sequences, the pheromone receptor responsible for the detection of (3Z,6Z,8E)-dodecatrien-1-ol should be the preferential target of future deorphanisation efforts. This compound became the most widespread component of termite TFPs and SPPs (Bordereau & Pasteels, 2011 [↗](#); Sillam-Dussès, 2010 [↗](#)). It occurs in most lineages of Neoisoptera and is characteristic by extraordinary efficiency as evidenced by strikingly low activity threshold. In some species, 10^{-5} ng/cm of the trail is sufficient to elicit the trail-following behavior, while the activity thresholds for other known TFPs are by two or more orders of magnitude higher (Bordereau & Pasteels, 2011 [↗](#)). In *P. simplex*, (3Z,6Z,8E)-dodecatrien-1-ol occurs not only as a minor component of TFP, but also as the main component of SPP, emitted by dispersing female in tiny quantities, which are sufficient to mediate the appropriate antennal and behavioral response of males.

An intuitive target for future functional analysis is *PsimOR15*, the likely tandem copy paralog of *PsimOR14*. Both genes are localized on the same locus, share the gene architecture, and their transcripts are equally represented in worker antennal transcriptome, though *PsimOR15* does not display the caste-biased expression. *PsimOR15* is thus a candidate for potential pheromone receptor function.

Materials and methods

Termites

Multiple laboratory colonies of *P. simplex*, originating from previous field collections in Cuba and Florida, are held in the Institute of Organic Chemistry and Biochemistry, Czech Academy of Sciences. Colonies are reared in glass vivaria at 27°C and 80% relative humidity in clusters of spruce wood slices. These colonies were used for RNA extraction, single sensillum recordings

(SSR), electroantennographic recordings (EAG), and scanning electron microscopy (SEM). For all experiments, workers of 4th or 5th stage were selected as the most abundant developmental stages, recognized according to body size and head width.

RNA extraction, OR cloning and construct generation

Total RNA was extracted from 20 pairs of dissected *P. simplex* antennae using PureLink RNA Mini Kit (Invitrogen, Carlsbad, CA, USA) following the manufacturer's protocol and quantified using NanoDrop spectrophotometer (Thermo, Delaware, USA). From the total RNA, 2 µg was used to synthesize the cDNA using SuperScript IV Reverse Transcriptase (Invitrogen, Carlsbad, CA, USA) according to manufacturer's instructions. The efficiency of cDNA synthesis was evaluated by amplification of odorant receptor co-receptor (ORCo). The list of primers is provided in Supplementary Table S17).

The full-length open reading frame (ORF) of each selected PsimORs was PCR-amplified from the cDNA using the DreamTaq Green PCR Master Mix (Invitrogen, USA) and gene-specific primers (Supplementary Table S17). Amplification products were purified by QIAquick Gel Extraction Kit (Qiagen, Germany), cloned into pCR8/GW/TOPO vector using the TOPO TA Cloning Kit (Invitrogen, USA) and transformed into OneShot TOP10 competent cells (Invitrogen, USA). Positive colonies were selected based on colony-PCRs using primers GW1 and GW2, recombinant plasmids were isolated using the QIAprep 2.0 Spin Miniprep Columns (Qiagen, Germany) and sequences were verified by Sanger sequencing (Eurofins Genomics, Germany).

The expression vector constructs were prepared using the Gateway LR recombination cloning technology (Invitrogen, USA) based on recombination of the phage-like attachment sites attL/R in pCR8/GW/TOPO with the bacteria-like attachment site attB in pUASg.attB vector (obtained from *Drosophila* Genomics Resource Center, Bloomington, USA). The resulting constructs pUASg.attB-PsimOR were purified using the QIAprep 2.0 Spin Miniprep Columns (Qiagen, Germany) and insert sequences were verified by Sanger sequencing at Eurofins Genomics (Germany). All primers used for Sanger sequencing and colony-PCR are listed in Supplementary Table S17).

Fly lines

D. melanogaster lines used in the Empty Neuron system were kindly provided by Dr. Thomas O. Auer (from Richard Benton Lab, University of Lausanne, Switzerland). The wild type *W*¹¹¹⁸ line, used as a control, was kindly provided by Prof. Michal Žurovec (Biology Centre, Czechia). All *Drosophila melanogaster* lines were reared in an incubator which was set at 24±2°C with relative humidity of 50±5%. Flies were fed with in-house prepared diet based on standard cornmeal food. The fly lines used are listed in Supplementary Table S18.

Transgenic expression of termite

ORs in *D. melanogaster* ab3A neuron

Selected PsimORs were expressed in the *Drosophila melanogaster* Empty Neuron system for functional screening. Transgenic *D. melanogaster* UAS-PsimOR lines were generated by BestGene Inc. (Chino Hills, CA, USA) by injecting pUASg.attB-PsimOR vectors into fly embryos expressing the integrase PhiC31 and carrying an attP landing site resulting in flies with genotype w⁻; +; UAS-PsimOR (w⁺)/+.

The recent CRISPR-Cas9-engineered empty neuron line Or22ab^{-Gal4} (Chahda et al., 2019 [DOI](#)) was used as Δhalo genetic background for the expression of UAS-PsimOR in Dmel ab3 sensilla. The fly crossing scheme was adapted from (Gonzalez et al., 2016 [DOI](#)) with a modification at the F3 crossing. Final homozygote lines with UAS-PsimOR and Or22ab^{-Gal4} were generated and used for the electrophysiological recordings. The full description of the crossing scheme is provided in Supplementary Fig. S2.

Chemicals

For SSR measurements, we used a total of 73 chemicals organized into four panels. The main panel contained 17 compounds biologically relevant to termites, i.e. components of termite pheromones and cuticular hydrocarbons known from Neoisoptera and structurally related compounds. This panel was used for initial SSR screening of PsimOR9, 14, 30 and 31 in transgenic *D. melanogaster* and for SSR experiments with *P. simplex* workers. For detailed analysis of Psim OR14, three additional panels were used, consisting of 56 frequently occurring insect semiochemicals (e.g., terpenoids, fatty acid esters, fatty alcohols and aldehydes, etc.). Panel 1 compounds were diluted in *n*-hexane to 100 ng/μl, panel 2–4 compounds were diluted in paraffin oil to 10⁻³ v/v. List of all compounds tested and their origin are listed in Supplementary Table S19.

Organic synthesis

For the purpose of SSR experiments, we synthesized (Z)-dodec-3-en-1-ol, (3Z,6Z)-dodeca-3,6-dien-1-ol, (3Z,6Z,8E)-dodecatrien-1-ol, and dodec-3-yn-1-ol, and included these compounds into Panel 1. The synthesis of these fatty alcohols is described in the Supplementary Information file.

Electrophysiology

SSR recordings on *Drosophila* ab3 sensillum were performed as described previously (Benton & Dahanukar, 2023 [DOI](#); Olsson & Hansson, 2013 [DOI](#)). We used 2–4 days old flies for one recording per each to avoid neuronal adaptations from multiple stimulations. To expose more ab3 sensilla, the fly preparation was done with arista down (Keesey et al., 2022 [DOI](#)). In termites, the olfactory sensilla situated on the last antennal flagellomere of workers was targeted for SSR, since their number increases towards the distal end of termite antennae, the last segment being significantly more populated by olfactory sensilla than any other segment (Castillo et al., 2021 [DOI](#)). The antennal preparation was done similarly as described for *Drosophila* with the grounding electrode inserted into the clypeus. The sensilla were observed under the Nikon FN1 eclipse microscope at 60× magnification. For all electrophysiological measurements, the recording electrode was brought into contact with the base of the sensillum using a Kleindiek Nanotechnik MM3A micromanipulator connected to a cubic micromanipulator device. Using Syntech stimulus delivery system (CS55 model, Syntech, Germany), the odorant stimulus was administered as a 0.3 s pulse by inserting the tip of the glass Pasteur pipette through a hole in a tube carrying a purified air stream (0.4 L/min). The distance between the antenna and odor delivery system was approximately 4 cm. From each diluted odorant (100 ng/μL), 10 μl were pipetted on 1 cm diameter filter paper disk placed in a glass Pasteur pipette in the screening experiment, while the doses ranging from 0.01 to 500 ng of neocembrene per filter paper were used in the dose-response experiments.

The signal was amplified and digitally converted using Syntech IDAC-4. The neuronal cells were sorted based on their amplitude and the spikes were counted using the AutoSpike v3.9 software (Syntech Ockenfels, Germany). Δ spike was calculated by subtracting the number of spikes during 1 second post-stimulation from the number of spikes generated 1 second before the stimulation. In dose response experiments, the counting periods were 0.5 s. Δ spike values were corrected by subtracting the response generated by the solvent and converted into Δ spike/s (Benton & Dahanukar, 2023 [DOI](#); Olsson & Hansson, 2013 [DOI](#)). The receptor lifetime sparseness value was calculated according to Chang et al. (Chang et al., 2023 [DOI](#)).

EAG experiment addressing the caste-specificity of antennal responses to neocembrene was performed with 15 workers and 15 soldiers; each individual was only used for one stimulation series consisting of air–hexane–neocembrene (10 ng)–hexane–air. Brain and antennal tip were placed between two Ag/AgCl electrodes containing Ringer's solution and connected to a high impedance (10¹⁴ Ω) amplifier (Syntech, Buchenbach, Germany). The antennal preparation was placed into a stream of cleaned air (500 mL/min), into which the stimuli were injected from

Pasteur pipettes containing a 1.5 cm² filter paper impregnated with 10 µL of the tested solution. Odor injections were controlled by a foot switch-operated Syntech stimulus controller and maximal negative deflection was measured using Syntech EagPro software. Pasteur pipettes containing odorant stimuli were changed after three stimulations. Air responses were used for data normalization, the responses log₂-transformed to reduce heteroscedasticity and comply with assumptions for parametric testing (Bartlett test for equal variances, and Shapiro-Wilk normality test), and then compared between workers and soldiers using Student's t-test.

Scanning electron microscopy

For SEM, 10 workers with intact antennae were cold-anesthetized and decapitated with micro-scissors. Heads were desiccated in increasing ethanol concentrations (60, 80, 90, and 96%, each for 2 h) followed by 12 h in acetone. Heads were then attached to aluminium holders for microscopy using adhesive tape, and differentially oriented to allow axial, dorsal, ventral, and lateral views. The samples were gold-coated for regular SEM (4 nm gold layer) and high-resolution SEM (HR-SEM, 2 nm) using sputter coater Bal-Tec SCD 050. Last antennal segments were inspected and photographed under scanning electron microscope JEOL 6380 LV (SEM). Surface of particular sensilla were studied using high resolution field emission scanning electron microscope JSM-IT800 (HR-SEM) and Olympus Soft Imaging Solution software. Working distance for all samples was 4.0–4.1 mm and accelerating voltage 2.0 kV.

Bioinformatics

For phylogenetic reconstruction of termite ORs, we used 182 OR protein sequences originating from five termite species, i.e. *Neotermes cubanus*, *Prorethitermes simplex*, *Inquilinitermes inquilinus* (Johny et al., 2023 [↗](#)), *Zootermopsis nevadensis* (Terrapon et al., 2014 [↗](#)) and *Cryptotermes secundus* (Harrison et al., 2018 [↗](#)), and the bristletail *Lepisma saccharina* (Thoma et al., 2019 [↗](#)) as a basal insect outgroup. For all species also the ORCo sequence was included. Sequences were aligned by means of the MUSCLE algorithm and used for reconstruct the phylogenetic tree with the IQ-TREE maximum likelihood algorithm (Nguyen et al., 2015 [↗](#)) using the JTT+F+R8 substitution model and 10,000 ultrafast bootstrap replicates.

The gene structures of PsimORs were characterized by local alignment of full-length transcript sequences from Johny et al. (Johny et al., 2023 [↗](#)) to our in-house genome assembly using BLAST (for details on genome assembly see Koubová et al., 2021 [↗](#)) and confirmed with genomic mapping of the RNAseq data from *P. simplex* antennae available under accession SRX17749141 in NCBI SRA archives using STAR aligner v2.7.10b (Dobin et al., 2013 [↗](#)). The mapping results were further used for abundance estimations of all ORs and ORCo in antennal transcriptome reported in Johny et al. (Johny et al., 2023 [↗](#)). Read counts were obtained with featureCounts tool from the Subread package (<https://subread.sourceforge.net/> [↗](#)) and normalized according to the FPKM (Fragments Per Kilobase Million) method.

Differential OR expression analysis in *P. simplex* soldier and worker heads was performed using the RNAseq data available in SRA archives under accessions SRX18952230-32 and SRX18952237-39. Read counts obtained using STAR mapping and featureCounts estimations were statistically evaluated using the DESeq2 Bioconductor package in R and edgeR.

PsimOR14 secondary structure was predicted using online tools Jpred 4.0.0 (www.compbio.dundee.ac.uk/jpred [↗](#)) and TMHMM2.0 (<https://services.healthtech.dtu.dk/services/TMHMM-2.0> [↗](#)), schematic model was generated using Protter (<https://wlab.ethz.ch/protter> [↗](#)).

Conflict of interests

The authors declare no competing interests.

Author contributions

SD – SSR, fly transgenesis; OL – bioinformatics; SD, JJ – fly transgenesis; KK – EAG; JK – insect culture, SEM; JN – SEM, HR-SEM; DSD – advising; PK – chemical analysis; JV, JŠ – molecular dynamics; RH, EGW, OL, SD – conception, supervision, statistics, writing. All authors contributed to the manuscript writing and approved its final version.

Data availability

Nucleotide and protein sequences of termite ORs used for phylogenetic reconstruction and functional characterizations were published in Johnny et al. (Johnny et al., 2023 [DOI](#)) and the raw sequencing data was previously deposited in NCBI SRA archive as PRJNA885453 bioproject. Transcript abundances of *P. simplex* ORs were also inferred from the antennal transcriptome data, available at NCBI under SRX17749141. Sequences of PsimOR14 studied in detail in the present paper are listed in the Supplementary Table S12 and deposited at NCBI as OR921181 entry. Origin of the *P. simplex* draft genome assembly is reported in Koubová et al. (2021) [DOI](#). Differential expression of *P. simplex* ORs in workers and soldiers was studied using caste-specific head transcriptomes available at NCBI as SRA archives under accessions SRX18952230-32 and SRX18952237-39.

Acknowledgements

This study was supported by Czech Science Foundation (No. 20-17194S) and Institute of Organic Chemistry and Biochemistry, CAS (RVO: 61388963). We thank M. Hyliš and the Viničná Microscopy Core Facility (VMCF of the Faculty of Science, Charles University) supported by the MEYS CR (LM2023050 Czech-BioImaging) for their support and assistance with microscopy techniques. We also thank Martina Hajdušková (www.biographix.cz [DOI](#)) for insect drawings used in **Fig. 1** [DOI](#).

References

- Andersson M. N., Löfstedt C., Newcomb R. D (2015) **Insect olfaction and the evolution of receptor tuning** *Front Ecol Evol* **3**
- Bagnères A. G., Hanus R, Aquiloni L, Tricarico E (2015) **Communication and social regulation in termites** *Social recognition in invertebrates* Springer International Publishing :193–248
- Benton R (2015) **Multigene family evolution: Perspectives from insect chemoreceptors** *Trends Ecol Evol* **30**:590–600
- Benton R., Dahanukar A (2023) **Chemosensory coding in Drosophila single sensilla** *Cold Spring Harb Protoc* **2023**
- Benton R., Sachse S., Michnick S. W., Vosshall L. B (2006) **Atypical membrane topology and heteromeric function of Drosophila odorant receptors in vivo** *PLoS Biol* **4**
- Benton R., Vannice K. S., Gomez-Diaz C., Vosshall L. B (2009) **Variant ionotropic glutamate receptors as chemosensory receptors in Drosophila** *Cell* **136**:149–162
- Bordereau C., Pasteels J. M, Bignell D. E., Roisin Y., Lo N. (2011) **Pheromones and chemical ecology of dispersal and foraging in termites** *Biology of termites: A modern synthesis* Springer :279–320
- Brand P., Robertson H. M., Lin W., Pothula R., Klingeman W. E., Jurat-Fuentes J. L., Johnson B. R (2018) **The origin of the odorant receptor gene family in insects** *Elife* **7**
- Buček A., Šobotník J., He S., Shi M., McMahon D. P., Holmes E. C., Roisin Y., Lo N., Bourguignon T (2019) **Evolution of termite symbiosis informed by transcriptome-based phylogenies** *Curr Biol* **29**:3728–3734
- Butterwick J. A., Del Marmol J., Kim K. H., Kahlson M. A., Rogow J. A., Walz T., Ruta V (2018) **Cryo-EM structure of the insect olfactory receptor Orco** *Nature* **560**:447–452
- Caminer M. A., Libbrecht R., Majoe M., Ho D. V., Baumann P., Foitzik S (2023) **Task-specific odorant receptor expression in worker antennae indicates that sensory filters regulate division of labor in ants** *Commun Biol* **6**
- Carey A. F., Wang G., Su C.-Y., Zwiebel L. J., Carlson J. R (2010) **Odorant reception in the malaria mosquito *Anopheles gambiae*** *Nature* **464**:66–71
- Castillo P., Husseneder C., Sun Q (2022) **Molecular characterization and expression variation of the odorant receptor co-receptor in the Formosan subterranean termite** *PLoS One* **17**
- Castillo P., Le N., Sun Q (2021) **Comparative antennal morphometry and sensilla organization in the reproductive and non-reproductive castes of the Formosan subterranean termite** *Insects* **12**

- Clyne P. J., Warr C. G., Freeman M. R., Lessing D., Kim J., Carlson J. R (1999) **A novel family of divergent seven-transmembrane proteins: candidate odorant receptors in *Drosophila*** *Neuron* **22**:327–338
- del Marmol J., Yedlin M. A., Ruta V (2021) **The structural basis of odorant recognition in insect olfactory receptors** *Nature* **597**:126–131
- Dobin A., Davis C. A., Schlesinger F., Drenkow J., Zaleski C., Jha S., Batut P., Chaisson M., Gingeras T. R (2013) **STAR: ultrafast universal RNA-seq aligner** *Bioinformatics* **29**:15–21
- Dolejšová K., Krasulová J., Kutalová K., Hanus R (2014) **Chemical alarm in the termite *Termitogeton planus* (Rhinotermitidae)** *J Chem Ecol* **40**:1269–1276
- Engsontia P., Sangket U., Robertson H. M., Satasook C (2015) **Diversification of the ant odorant receptor gene family and positive selection on candidate cuticular hydrocarbon receptors** *BMC Res Notes* **8**
- Evangelista Dominic A., Wipfler B., Béthoux O., Donath A., Fujita M., Kohli Manpreet K., Legendre F., Liu S., Machida R., et al. (2019) **An integrative phylogenomic approach illuminates the evolutionary history of cockroaches and termites (Blattodea)** *Proc Roy Soc B: Biol Sci* **286**
- Fleischer J., Krieger J (2018) **Insect pheromone receptors – Key elements in sensing intraspecific chemical signals** *Frontiers Cell Neurosci* **12**
- Gao Y., Huang Q., Xu H (2020) **Silencing Orco impaired the ability to perceive trail pheromones and affected locomotion behavior in two termite species** *J Econ Entomol* **113**:2941–2949
- Gomez Ramirez W. C., Thomas N. K. T., Muktar I. J., Riabinina O (2023) **The neuroecology of olfaction in bees** *Curr Opin Insect Sci* **56**
- Gonzalez F., Witzgall P., Walker W. B (2016) **Protocol for heterologous expression of insect odourant receptors in *Drosophila*** *Front Ecol Evol* **4**
- Gössinger E., Kinghorn A. D., Falk H., Gibbons S., i J., Kobayashi Y. Asakawa, Liu J.-K. (2019) **Chemistry of the secondary metabolites of termites** *Progress in the Chemistry of organic natural products* Springer International Publishing :1–384
- Guo X., Yu Q., Chen D., Wei J., Yang P., Yu J., Wang X., Kang L (2020) **4-Vinylanisole is an aggregation pheromone in locusts** *Nature* **584**:584–588
- Hanus R., Šobotník J., Valterová I., Lukáš J (2006) **The ontogeny of soldiers in *Prorhinotermes simplex* (Isoptera, Rhinotermitidae)** *Insectes Soc* **53**:249–257
- Hanus R., Luxová A., Šobotník J., Kalinová B., Jiroš P., Křeček J., Bourguignon T., Bordereau C (2009) **Sexual communication in the termite *Prorhinotermes simplex* (Isoptera, Rhinotermitidae) mediated by a pheromone from female tergal glands** *Insectes Soc* **56**:111–118
- Harrison M. C., Jongepier E., Robertson H. M., Arning N., Bitard-Feildel T., Chao H., Childers C. P., Dinh H., Doddapaneni H., et al. (2018) **Hemimetabolous genomes reveal molecular basis of termite eusociality** *Nat Ecol Evol* **2**:557–566

- Chahda J. S., Soni N., Sun J. S., Ebrahim S. A. M., Weiss B. L., Carlson J. R (2019) **The molecular and cellular basis of olfactory response to tsetse fly attractants** *PLoS Genet* **15**
- Chang H., Unni A. P., Tom M. T., Cao Q., Liu Y., Wang G., Llorca L. C., Brase S., Bucks S., et al. (2023) **Odorant detection in a locust exhibits unusually low redundancy** *Curr Biology* **33**:5427–5438
- Jirošová A., Jančařík A., Menezes R. C., Bazalová O., Dolejšová K., Vogel H., Jedlička P., Buček A., Brabcová J., et al. (2017) **Co-option of the sphingolipid metabolism for the production of nitroalkene defensive chemicals in termite soldiers** *Insect Biochem Mol Biol* **82**:52–61
- Johny J., Diallo S., Lukšan O., Shewale M., Kalinová B., Hanus R., Große-Wilde E (2023) **Conserved orthology in termite chemosensory gene families** *Front Ecol Evol* **10**
- Jongepier E., Séguret A., Labutin A., Feldmeyer B., Gstöttl C., Foitzik S., Heinze J., Bornberg-Bauer E (2022) **Convergent loss of chemoreceptors across independent origins of slave-making in ants** *Mol Biol Evol* **39**
- Kaib M., Veeresh G. K., Mallik B., Viraktamath C. A. (1990) **Multiple functions of exocrine secretions in termite communication: exemplified by *Schedorhinotermes lamanianus*** *Social insects and the environment* E. J. Brill :37–38
- Keesey I. W., Zhang J., Depetris-Chauvin A., Obiero G. F., Gupta A., Gupta N., Vogel H., Knaden M., Hansson B. S. (2022) **Functional olfactory evolution in *Drosophila suzukii* and the subgenus *Sophophora*** *iScience* **25**
- Koubová J., Pangráčová M., Jankásek M., Lukšan O., Jehlík T., Brabcová J., Jedlička P., Křivánek J., Čapková Frydrychová R., Hanus R (2021) **Long-lived termite kings and queens activate telomerase in somatic organs** *Proc Roy Soc B: Biol Sci* **288**
- Larsson M. C., Domingos A. I., Jones W. D., Chiappe M. E., Amrein H., Vosshall L. B (2004) **Or83b encodes a broadly expressed odorant receptor essential for *Drosophila* olfaction** *Neuron* **43**:703–714
- Legan A. W., Jernigan C. M., Miller S. E., Fuchs M. F., Sheehan M. J (2021) **Expansion and accelerated evolution of 9-exon odorant receptors in polistes paper wasps** *Mol Biol Evol* **38**:3832–3846
- Leonhardt Sara D., Menzel F., Nehring V., Schmitt T (2016) **Ecology and evolution of communication in social insects** *Cell* **164**:1277–1287
- McKenzie S. K., Fetter-Prunedo I., Ruta V., Kronauer D. J. C (2016) **Transcriptomics and neuroanatomy of the clonal raider ant implicate an expanded clade of odorant receptors in chemical communication** *Proc Natl Acad Sci USA* **113**:14091–14096
- Mitaka Y., Akino T (2021) **A review of termite pheromones: Multifaceted, context-dependent, and rational chemical communications** *Front Ecol Evol* **8**
- Mitaka Y., Kobayashi K., Mikheyev A., Tin M. M. Y., Watanabe Y., Matsuura K (2016) **Caste-specific and sex-specific expression of chemoreceptor genes in a termite** *PLoS One* **11**
- Nei M., Rooney A. P (2005) **Concerted and birth-and-death evolution of multigene families** *Annu Rev Genet* **39**:121–152

- Nguyen L. T., Schmidt H. A., von Haeseler A., Minh B. Q. (2015) **IQ-TREE: a fast and effective stochastic algorithm for estimating maximum-likelihood phylogenies** *Mol Biol Evol* **32**:268–274
- Obiero G. F., Pauli T., Geuverink E., Veenendaal R., Niehuis O., Große-Wilde E (2021) **Chemoreceptor diversity in apoid wasps and its reduction during the evolution of the pollen-collecting lifestyle of bees (Hymenoptera: Apoidea)** *Genome Biol Evol* **13**
- Olsson S. B., Hansson B. S., Touhara K. (2013) **Electroantennogram and single sensillum recording in insect antennae** *Pheromone Signaling: Methods and Protocols* Humana Press :157–177
- Pask G. M., Slone J. D., Millar J. G., Das P., Moreira J. A., Zhou X. F., Bello J., Berger S. L., Bonasio R., et al. (2017) **Specialized odorant receptors in social insects that detect cuticular hydrocarbon cues and candidate pheromones** *Nat Commun* **8**
- Pettersson J. H., Cattaneo A. M (2023) **Heterologous investigation of metabotropic and ionotropic odorant receptors in ab3A neurons of Drosophila melanogaster** *Front Mol Biosci* **10**
- Piskorski R., Hanus R., Vašíčková S., Cvačka J., Šobotník J., Svatoš A., Valterová I (2007) **Nitroalkenes and sesquiterpene hydrocarbons from the frontal gland of three Prorhinotermes termite species** *J Chem Ecol* **33**:1787–1794
- Robertson H. M (2019) **Molecular evolution of the major arthropod chemoreceptor gene families** *Annu Rev Entomol* **64**:227–242
- Robertson H. M., Baits R. L., Walden K. K. O., Wada-Katsumata A., Schal C (2018) **Enormous expansion of the chemosensory gene repertoire in the omnivorous German cockroach Blattella germanica** *J Exp Zool B Mol Dev Evol* **330**:265–278
- Roisin Y., Everaerts C., Pasteels J. M., Bonnard O (1990) **Caste-dependent reactions to soldier defensive secretion and chiral alarm/recruitment pheromone in Nasutitermes princeps** *J Chem Ecol* **16**:2865–2875
- Rupf T., Roisin Y (2008) **Coming out of the woods: do termites need a specialized worker caste to search for new food sources?** *Naturwissenschaften* **95**:811–819
- Sato K., Pellegrino M., Nakagawa T., Nakagawa T., Voss hall L. B., Touhara K (2008) **Insect olfactory receptors are heteromeric ligand-gated ion channels** *Nature* **452**:1002–1006
- Sillam-Dussès D. (2010) **Trail pheromones and sex pheromones in termites** Nova Novinka, Nova Science Publishers
- Sillam-Dussès D., Kalinová B., Jiroš P., Březinová A., Cvačka J., Hanus R., Šobotník J., Bordereau C., Valterová I (2009) **Identification by GC-EAD of the two-component trail-following pheromone of Prorhinotermes simplex (Isoptera, Rhinotermitidae, Prorhinotermitinae)** *J Insect Physiol* **55**:751–757
- Slone J. D., Pask G. M., Ferguson S. T., Millar J. G., Berger S. L., Reinberg D., Liebig J., Ray A., Zwiebel L. J (2017) **Functional characterization of odorant receptors in the ponerine ant, Harpegnathos saltator** *Proc Natl Acad Sci USA* **114**:8586–8591

- Šobotník J., Hanus R., Kalinová B., Piskorski R., Cvačka J., Bourguignon T., Roisin Y (2008) **(E,E)-alpha-farnesene, an alarm pheromone of the termite *Proterhinotermes canalifrons*** *J Chem Ecol* **34**:478–86
- Šobotník J., Jirošová A., Hanus R (2010) **Chemical warfare in termites** *J Insect Physiol* **56**:1012–21
- Steiger S., Schmitt T., Schaefer H. M (2010) **The origin and dynamic evolution of chemical information transfer** *Proc Roy Soc B: Biol Sci* **278**:970–979
- Terrapon N., Li C., Robertson H. M., Ji L., Meng X., Booth W., Chen Z., Childers C. P., Glastad K. M., et al. (2014) **Molecular traces of alternative social organization in a termite genome** *Nat Commun* **5**
- Thoma M., Missbach C., Jordan M. D., Grosse-Wilde E., Newcomb R. D., Hansson B. S (2019) **Transcriptome surveys in silverfish suggest a multistep origin of the insect odorant receptor gene family** *Front Ecol Evol* **7**
- Traniello J. F. A (1981) **Enemy deterrence in the recruitment strategy of a termite: soldier-organized foraging in *Nasutitermes costalis*** *Proc Natl Acad Sci USA* **78**:1976–1979
- Traniello J. F. A., Busher C (1985) **Chemical regulation of polyethism during foraging in the Neotropical termite *Nasutitermes costalis*** *J Chem Ecol* **11**:319–332
- Wanner K. W., Nichols A. S., Walden K. K., Brockmann A., Luetje C. W., Robertson H. M (2007) **A honey bee odorant receptor for the queen substance 9-oxo-2-decenoic acid** *Proc Natl Acad Sci USA* **104**:14383–14388
- Wicher D., Schafer R., Bauernfeind R., Stensmyr M. C., Heller R., Heinemann S. H., Hansson B. S (2008) **Drosophila odorant receptors are both ligand-gated and cyclic-nucleotide-activated cation channels** *Nature* **452**:1007–1011
- Yan H., Jafari S., Pask G., Zhou X., Reinberg D., Desplan C (2020) **Evolution, developmental expression and function of odorant receptors in insects** *J Exp Biol* **223**
- Yuvaraj J. K., Roberts R. E., Sonntag Y., Hou X.-Q., Grosse-Wilde E., Machara A., Zhang D.-D., Hansson B. S., Johanson U., et al. (2021) **Putative ligand binding sites of two functionally characterized bark beetle odorant receptors** *BMC Biology* **19**
- Zhang R.-B., Liu Y., Yan S.-C., Wang G.-R (2019) **Identification and functional characterization of an odorant receptor in pea aphid, *Acyrtosiphon pisum*** *Insect Sci* **26**:58–67
- Zhang R., Wang B., Grossi G., Falabella P., Liu Y., Yan S., Lu J., Xi J., Wang G (2017) **Molecular basis of alarm pheromone detection in aphids** *Curr Biol* **27**:55–61
- Zhou X., Rokas A., Berger S. L., Liebig J., Ray A., Zwiebel L. J (2015) **Chemoreceptor evolution in Hymenoptera and its implications for the evolution of eusociality** *Genome Biol Evol* **7**:2407–2416

Editors

Reviewing Editor

Hiromu Tanimoto

Tohoku University, Sendai, Japan

Senior Editor

Albert Cardona

University of Cambridge, Cambridge, United Kingdom

Reviewer #1 (Public review):

Summary:

In their comprehensive analysis Diallo et al. deorphanise the first olfactory receptor of a non-hymenopteran eusocial insect - a termite and identified the well-established trail pheromone neocembrene as the receptor's best ligand. By using a large set of odorants the authors convincingly show that, as expected for a pheromone receptor, PsimOR14 is very narrowly tuned. While the authors first make use of an ectopic expression system, the empty neuron of *Drosophila melanogaster*, to characterise the receptor's responses, they next perform single sensillum recordings with different sensilla types on the termite antenna. By that, they are able to identify a sensillum that houses three neurons, of which the B neuron exhibits the narrow responses described for PsimOR14. Hence the authors do not only identify the first pheromone receptor in a termite but can even localize its expression on the antenna. The authors in addition perform a structural analysis to explain the binding properties of the receptor and its major and minor ligands (as this is beyond my expertise, I cannot judge this part of the manuscript). Finally, they compare expression patterns of ORs in different castes and find that PsimOR14 is more strongly expressed in workers than in soldier termites, which corresponds well with stronger antennal responses in the worker caste.

Strengths:

The manuscript is well-written and a pleasure to read. The figures are beautiful and clear. I actually had a hard time coming up with suggestions.

Weaknesses:

Whenever it comes to the deorphanization of a receptor and its potential role in behaviour (in the case of the manuscript it would be trail-following of the termite) one thinks immediately of knocking out the receptor to check whether it is necessary for the behaviour. However, I definitely do not want to ask for this (especially as the establishment of CRISPR Cas-9 in eusocial insects usually turns out to be a nightmare). I also do not know either, whether knockdowns via RNAi have been established in termites, but maybe the authors could consider some speculation on this in the discussion.

<https://doi.org/10.7554/eLife.101814.1.sa2>

Reviewer #2 (Public review):

Summary:

In this manuscript, the authors performed the functional analysis of odorant receptors (ORs) of the termite *Prorethia simplex* to identify the receptor of trail-following pheromone. The authors performed single-sensillum recording (SSR) using the transgenic *Drosophila* flies

expressing a candidate of the pheromone receptor and revealed that PsimOR14 strongly responds to neocembrene, the major component of the pheromone. Also, the authors found that one sensillum type (S I) detects neocembrene and also performed SSR for S I in wild termite workers. Furthermore, the authors revealed the gene, transcript, and protein structures of PsimOR14, predicted the 3D model and ligand docking of PsimOR14, and demonstrated that PsimOR14 is higher expressed in workers than soldiers using RNA-seq for heads of workers and soldiers of *P. simplex* and that EAG response to neocembrene is higher in workers than soldiers. I consider that this study will contribute to further understanding of the molecular and evolutionary mechanisms of the chemoreception system in termites.

Strength:

The manuscript is well written. As far as I know, this study is the first study that identified a pheromone receptor in termites. The authors not only present a methodology for analyzing the function of termite pheromone receptors but also provide important insights in terms of the evolution of ligand selectivity of termite pheromone receptors.

Weakness:

As you can see in the "Recommendations to the Authors" section below, there are several things in this paper that are not fully explained about experimental methods. Except for this point, this paper appears to me to have no major weaknesses.

<https://doi.org/10.7554/eLife.101814.1.sa1>

Reviewer #3 (Public review):

Summary:

Chemical communication is essential for the organization of eusocial insect societies. It is used in various important contexts, such as foraging and recruiting colony members to food sources. While such pheromones have been chemically identified and their function demonstrated in bioassays, little is known about their perception. Excellent candidates are the odorant receptors that have been shown to be involved in pheromone perception in other insects including ants and bees but not termites. The authors investigated the function of the odorant receptor PsimOR14, which was one of four target odorant receptors based on gene sequences and phylogenetic analyses. They used the *Drosophila* empty neuron system to demonstrate that the receptor was narrowly tuned to the trail pheromone neocembrene. Similar responses to the odor panel and neocembrene in antennal recordings suggested that one specific antennal sensillum expresses PsimOR14. Additional protein modeling approaches characterized the properties of the ligand binding pocket in the receptor. Finally, PsimOR14 transcripts were found to be significantly higher in worker antennae compared to soldier antennae, which corresponds to the worker's higher sensitivity to neocembrene.

Strengths:

The study presents an excellent characterization of a trail pheromone receptor in a termite species. The integration of receptor phylogeny, receptor functional characterization, antennal sensilla responses, receptor structure modeling, and transcriptomic analysis is especially powerful. All parts build on each other and are well supported with a good sample size.

Weaknesses:

The manuscript would benefit from a more detailed explanation of the research advances this work provides. Stating that this is the first deorphanization of an odorant receptor in a clade is insufficient. The introduction primarily reviews termite chemical communication

and deorphanization of olfactory receptors previously performed. Although this is essential background, it lacks a good integration into explaining what problem the current study solves.

Selecting target ORs for deorphanization is an essential step in the approach. Unfortunately, the process of choosing these ORs has not been described. Were the authors just lucky that they found the correct OR out of the 50, or was there a specific selection process that increased the probability of success?

The authors assigned antennal sensilla into five categories. Unfortunately, they did not support their categories well. It is not clear how they were able to differentiate SI and SII in their antennal recordings.

The authors used a large odorant panel to determine receptor tuning. The panel included volatile polar compounds and non-volatile non-polar hydrocarbons. Usually, some heat is applied to such non-volatile odorants to increase volatility for receptor testing. It is unclear how it is possible that these non-volatile compounds can reach the tested sensilla without heat application.

<https://doi.org/10.7554/eLife.101814.1.sa0>